

Metal-to-Insulator Crossover in the Low-Temperature Normal State of $\text{Bi}_2\text{Sr}_{2-x}\text{La}_x\text{CuO}_{6+\delta}$

S. Ono,¹ Yoichi Ando,^{1,2,*} T. Murayama,^{1,2,†} F. F. Balakirev,³ J. B. Betts,³ and G. S. Boebinger³

¹Central Research Institute of Electric Power Industry, Komae, Tokyo 201-8511, Japan

²Department of Physics, Science University of Tokyo, Shinjuku-ku, Tokyo 162-8601, Japan

³NHMFL, Los Alamos National Laboratory, Los Alamos, NM 87545

(November 9, 2018)

We measure the normal-state in-plane resistivity of $\text{Bi}_2\text{Sr}_{2-x}\text{La}_x\text{CuO}_{6+\delta}$ single crystals at low temperatures by suppressing superconductivity with 60-T pulsed magnetic fields. With decreasing hole doping, we observe a crossover from a metallic to insulating behavior in the low-temperature normal state. This crossover is estimated to occur near 1/8 doping, well inside the *underdoped* regime, and not at optimum doping as reported for other cuprates. The insulating regime is marked by a logarithmic temperature dependence of the resistivity over two decades of temperature, suggesting that a peculiar charge localization is common to the cuprates.

PACS numbers: 74.25.Dw, 74.25.Fy, 74.72.Hs

The normal-state of the high- T_c cuprate superconductors exhibits unusual properties thought to evidence non-Fermi-liquid behavior [1]. A sufficiently-intense magnetic field can suppress the superconducting phase and reveal the low-temperature limiting behavior in this strongly-correlated electron system [2,3]. For example, a metal-to-insulator (MI) crossover takes place at optimum doping in the normal state of the hole-doped $\text{La}_{2-y}\text{Sr}_y\text{CuO}_4$ (LSCO) system [3], implying that superconductivity in the underdoped regime may be realized in an otherwise-insulating system.

Recently, it was reported that a MI crossover also takes place at optimum doping in the electron-doped $\text{Pr}_{2-x}\text{Ce}_x\text{CuO}_{4+\delta}$ (PCCO) system [4]. If a MI crossover near optimum doping is a universal feature of all the cuprates, one plausible conclusion is that there is a quantum critical point at optimum doping, which might be the source of the non-Fermi-liquid behavior in the cuprates [5]. To date, however, only two systems have been systematically studied.

Surprisingly, the insulating behavior in both LSCO and PCCO is characterized by the in-plane resistivity $\rho_{ab}(T)$ increasing as $\log(1/T)$ [2,4,6]. This apparently diverging resistivity is sufficiently weak that it is experimentally difficult to precisely establish its functional form. Measurements on LSCO currently offer the best experimental case for a strict $\log(1/T)$ behavior with no evidence of saturation at low temperatures [2,6]. The data from PCCO do not span such a large dynamic range and tend toward saturation below ~ 3 K [4]. Because the $\log(1/T)$ divergence is not attributable to any known localization mechanism [2,6,7], it attracts substantial theoretical interest. Questions remain regarding its universality among the cuprates.

$\text{Bi}_2\text{Sr}_{2-x}\text{La}_x\text{CuO}_{6+\delta}$ (BSLCO, or La-doped Bi-2201) is well-suited for a systematic study of the low-temperature normal state because the carrier concentration can be

tuned in both the overdoped and underdoped regimes [8,9]. Also, since the maximum T_c of BSLCO is relatively low, superconductivity can be completely suppressed with experimentally-available 60-T pulsed magnetic fields. By suppressing superconductivity in a series of BSLCO single crystals, we measure ρ_{ab} in the normal state down to ~ 0.5 K. We find that in BSLCO the MI crossover, or the onset of localization, takes place not at optimum doping but well inside the underdoped regime. Hall measurements support the conclusion that the MI crossover occurs in BSLCO at approximately 1/8 hole concentration.

The single crystals of BSLCO are grown using a floating-zone technique over a wide range of La concentration $x = 0.23, 0.39, 0.66, 0.73, 0.76$ and 0.84 . Note that a larger x yields a more underdoped sample and $x=0.39$ is optimal-doping. The actual La concentration is measured by inductively-coupled plasma analysis and La homogeneity is confirmed by electron-probe microanalysis. For transport measurements, samples of $\sim 2 \times 1 \times 0.05$ mm³ are cut from large crystals. The thickness is accurately determined by weighing the samples with 0.1- μg resolution, which reduces the uncertainty in the absolute magnitude of ρ_{ab} to $\pm 5\%$ which results from the finite contact size. All the samples are annealed in flowing oxygen at 650°C for 48 hours to sharpen the superconducting transition, whose width (from dc magnetic susceptibility) is typically 2 K after annealing. The oxygen annealing also helps raise the optimum T_c ; the optimally-doped sample reported here shows zero-resistance at 38 K, the highest value ever reported for BSLCO and almost equal to the optimum T_c of LSCO.

The magnetic field dependence of $\rho_{ab}(H)$ is measured at fixed temperatures with the same ~ 100 kHz four-probe technique described previously [2,3]. The pulsed magnetic field is applied parallel to the c axis to best suppress superconductivity. Two different pulsed magnets

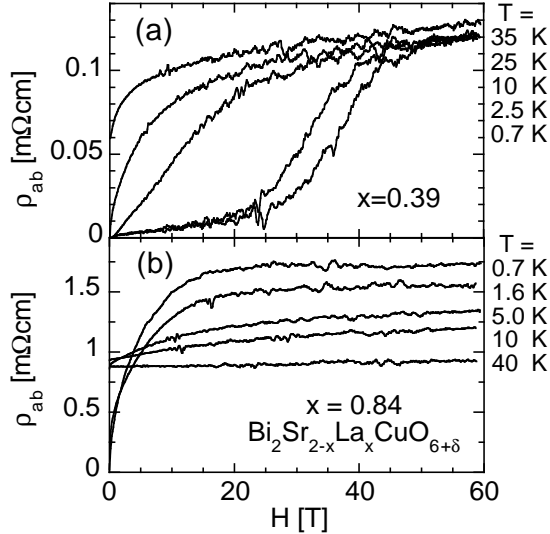


FIG. 1. Suppression of superconductivity by intense magnetic fields in BSLCO crystals with (a) $x=0.39$ and (b) $x=0.84$ at selected temperatures.

were utilized in these experiments: a 60-T magnet with a 15 msec pulse duration and a “long-pulse” 40-T magnet with a 500 msec pulse duration. Eddy-current heating, proportional to $(dH/dt)^2$, does not adversely affect the data, as confirmed by comparing data from the two different magnets and from pulses with different peak fields.

Figure 1 shows representative traces of $\rho_{ab}(H)$ at selected temperatures for $x = 0.39$, the optimally-doped sample, and $x = 0.84$, the most underdoped sample studied. Note that 60-T is sufficient to suppress superconductivity in BSLCO, even at optimum doping. Because the magnetoresistance in the normal state is negligible, we consider that the 60-T data represents the normal-state behavior at temperatures below T_c .

Figure 2 shows the T dependence of ρ_{ab} in 0 and 60 T for the six x values. In zero field (solid lines), all samples are metallic ($d\rho_{ab}/dT \geq 0$) above T_c except for the $x=0.84$ sample, in which the carrier concentration is sufficiently low that the superconducting phase has nearly disappeared. However, the 60-T data (symbols) reveal that the two most heavily underdoped samples, $x=0.84$ and 0.76, both show a strong increase in ρ_{ab} at low temperatures. As is most clear in the inset to Fig. 2, the $x=0.73$ sample shows a very weak upturn below 6K, which we interpret as the onset of localizing behavior in BSLCO. In contrast, $\rho_{ab}(T)$ for the $x=0.66$ sample is essentially constant below 10 K. The weak upturn in the $x=0.73$ sample makes it difficult to precisely determine the La concentration at the boundary for the onset of localization in the low-temperature normal state of BSLCO; however, clearly metallic behavior is found at $x=0.66$ in an underdoped sample with $T_c = 23$ K and, thus, the MI crossover in BSLCO appears to lie in the underdoped regime, not at optimum doping as in LSCO

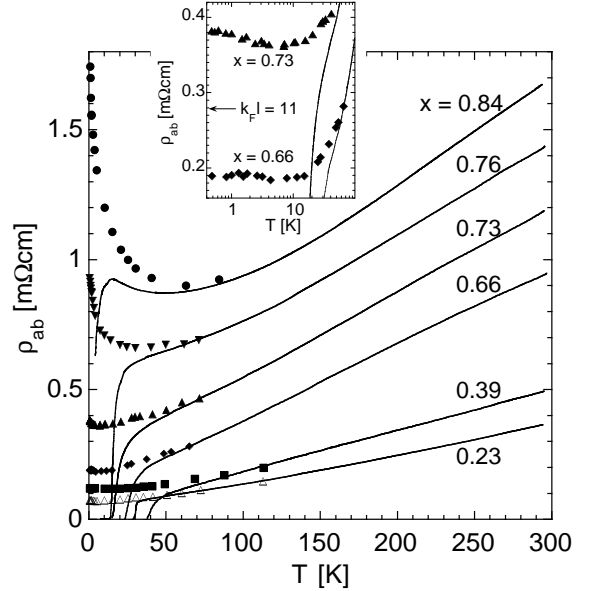


FIG. 2. Temperature dependence of ρ_{ab} for the BSLCO crystals in 0 T (solid lines) and in 60 T (symbols) for different La concentration x . The inset offers a clearer view of the low-temperature behaviors of the $x=0.73$ and 0.66 samples.

and PCCO.

Figure 3 contains selected BSLCO data from Fig. 2 replotted (filled circles) versus the logarithm of the temperature. Note that the low-temperature data for $x=0.84$ increases as $\log(1/T)$ with decreasing temperature. To determine whether this pronounced $\log(1/T)$ behavior persists to our lowest achievable temperature, we remeasured this sample at $H=30$ T at 1.5 K and 0.3 K (open circles) using the 40 T long-pulse magnet. In the $x = 0.84$ sample, 30 T is sufficient to suppress superconductivity (Fig. 1b). These 30-T data are consistent with those from the 60-T pulses and the $\log(1/T)$ behavior is found to extend over two decades of temperature from 30 K to 0.3 K without any sign of saturation at low-temperatures. This constitutes evidence for a strictly $\log(1/T)$ divergence that is even stronger than has been reported in LSCO [2]. As in LSCO, this $\log(1/T)$ behavior occurs at resistivities on the metallic side of the Mott limit ($k_Fl=1$ corresponds to $\rho_{ab}\simeq 3.1$ mΩcm in BSLCO).

Figure 3 also includes $\rho_{ab}(T)$ data from LSCO (open squares), reproduced from Ref. [3]. The vertical axes used for plotting the LSCO and BSLCO data have been scaled to directly compare the resistivity per CuO_2 layer, ρ_{ab}/c_0 , where c_0 is the c -axis lattice spacing. This normalized resistivity is given in units of $(k_Fl)^{-1}$ on the left-most axis: $\rho_{ab}/c_0 = h/(e^2 k_F l)$, where k_F is the Fermi wave vector, and l is the mean free path [10]. Several points are worth noting: (a) Optimally-doped BSLCO ($x=0.39$) exhibits a lower normalized resistivity than optimally-doped LSCO. This might account for the strongly insulating behavior beginning further from

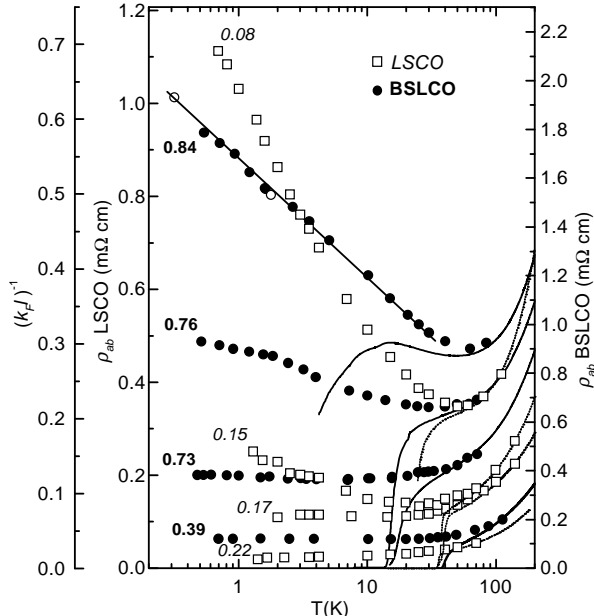


FIG. 3. Logarithmic plot of $\rho_{ab}(T)$ for BSLCO crystals in 0 T (solid lines) and in 60 T (filled circles), labelled by La concentration, x . The straight line emphasizes the $\log(1/T)$ behavior in the $x=0.84$ sample and open circles are 30-T data from the long-pulse magnet. LSCO data in 0 T (dashed lines) and in 60 T (open squares), labelled by Sr concentration, y , are from Ref. [3]. All data are vertically scaled to directly compare the resistivity per CuO_2 layer in units of $(k_F l)^{-1}$.

optimal-doping in BSLCO than in LSCO. (b) The LSCO and BSLCO data are consistent with the MI crossover occurring at a common value of normalized ρ_{ab} in the low-temperature limit, corresponding to $k_F l \simeq 12$, if the $x=0.73$ data are interpreted as insulating behavior. (c) The MI crossover occurs much more abruptly in LSCO (between $y = 0.15$ and 0.17) than in BSLCO. In BSLCO, the onset of localizing behavior occurs relatively gradually as the normalized $\rho_{ab}(T)$ becomes increasingly larger with increasing La concentration. (d) When comparing BSLCO and LSCO samples exhibiting similar normalized resistivities, the insulating behavior is stronger in LSCO than in BSLCO. This suggests that the normalized resistivity and estimated magnitude of $k_F l$ are not the sole factor determining the strength of the $\log(1/T)$ behavior in underdoped cuprates.

Developing a phase diagram for BSLCO is difficult because the hole concentration per Cu, p , cannot be chemically determined. Even if the La concentration, x , and excess oxygen, δ , are accurately known, the hole concentration p cannot be calculated because Bi-ion does not have a fixed valency [11]. We therefore estimate p for our BSLCO crystals based on Hall coefficient R_H . Figure 4 compares R_H from three different single-layer cuprates by normalizing with the unit cell volume V . Both the magnitude and the T -dependence of R_H/V of our optimally-doped BSLCO agree reasonably well with

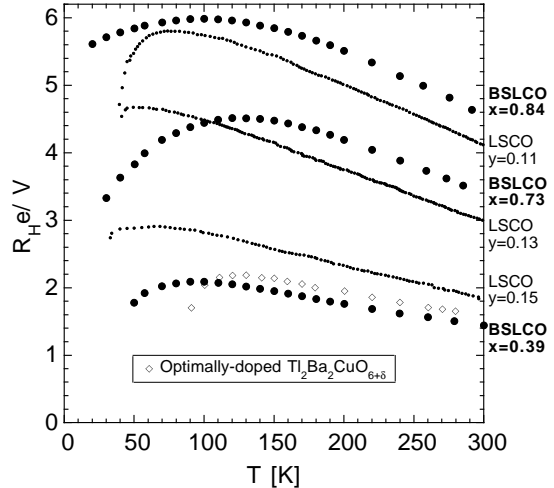


FIG. 4. Normalized Hall coefficient for several of our BSLCO samples, where e is the electronic charge and V is the unit cell volume. LSCO data are from Ref. [12] and optimally-doped $\text{Ti}_2\text{Ba}_2\text{CuO}_{6+\delta}$ data are from Ref. [13].

the optimally-doped ($y=0.15$) LSCO data [12] and the optimally-doped $\text{Ti}_2\text{Ba}_2\text{CuO}_{6+\delta}$ data [13]. From this, we conclude that our optimally-doped $x=0.39$ BSLCO sample has a hole concentration $p \simeq 0.15$. In LSCO, the p value is equal to the Sr concentration, y , which is used as a guide to estimate p for each of our BSLCO samples on the basis of the comparison of the R_H/V data. The approximate relationship between La concentration, x , and hole concentration, p , is given in Fig. 5.

Figure 5 contains the phase diagram resulting from our BSLCO transport data of Figs. 2 - 4. The zero-resistance superconducting transition temperatures T_c for our BSLCO samples is plotted (filled circles) versus La concentration x . The MI boundary, or the onset of the localizing behavior, in the normal state is schematically denoted by the open diamonds, the temperatures T_{min} where the $\rho_{ab}(T)$ shows a minimum in the 60-T data of Fig. 2. The top axis contains the approximate hole concentration p deduced from the Hall data of Fig. 4. It is clear from the phase diagram in Fig. 5 that the MI crossover at zero temperature lies well inside the underdoped regime for BSLCO, at a La concentration of $x \simeq 0.7$. The hole concentration at the MI crossover is estimated to be $p \simeq 1/8$.

Note that Fig. 5 suggests that the superconducting phase in BSLCO extends only down to $p \sim 0.10$, instead of $p \sim 0.05$ as with other hole-doped cuprates. This implies that the $x=0.84$ sample exhibits such a low T_c not because $p \sim 0.05$ but because T_c is reduced by disorder. This conclusion is supported by room-temperature thermopower measurements which are useful to independently estimate p in the cuprates [14]. We measure the thermopower of the BSLCO $x=0.84$ sample to be $38 \mu\text{V/K}$ at room temperature, a value much smaller than the $\sim 80 \mu\text{V/K}$ that would be expected at $p \sim 0.05$ [14].

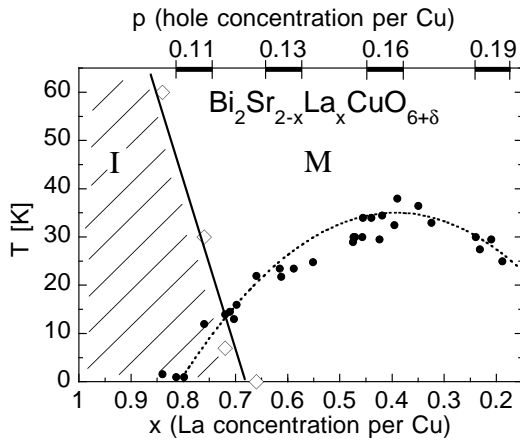


FIG. 5. Schematic phase diagram of BSLCO showing the superconducting T_c (solid circles) and T_{min} (open diamonds), the temperature at the minimum in ρ_{ab} . The solid line is boundary separating the insulating (I) and metallic (M) regimes. The top axis gives the approximate hole concentration corresponding to the measured La concentration.

Although the role of disorder is difficult to characterize, we note that disorder enhances insulating behavior in LSCO [6] and argue that increased disorder will likely expand the insulating regime. In other words, even though BSLCO crystals are disordered, less-disordered crystals are likely to exhibit a smaller insulating regime that recedes further into the underdoped regime. Hence, we believe the intrinsic behavior in BSLCO is that optimum doping occurs at $p \simeq 0.15$ and the insulating regime does not extend to optimum doping [15].

In LSCO, localizing behavior extends throughout the entire underdoped regime up to optimum doping [3]. Neutron scattering data on LSCO [17] suggests that charge is confined to stripes over the same range of carrier concentration: a plot of T_c versus incommensurability δ (Fig. 10 of Ref. [17]) finds a linear relation between T_c and δ that persists to $p=0.15$. Therefore, it is tempting to speculate that the $\rho_{ab} \sim \log(1/T)$ insulating behavior in LSCO might be associated with low dimensionality imposed by charge confinement onto stripes. If so, our transport data on BSLCO suggest that neutron scattering experiments will find the incommensurability, or the inverse separation between the stripes, to saturate for $p > 0.12$ in BSLCO. Additional transport studies on other hole-doped cuprates might further help establish general correlations between hole doping, stripe formation, and the unusual $\log(1/T)$ divergence of ρ_{ab} .

We note that the charge-stripe instability is often thought to be tied to the proximity to an antiferromagnetic ground state. A Néel transition has indeed been reported for heavily-La-doped Bi-2201 [8]. Also, recent theoretical arguments have linked the relatively low value of T_c at optimum doping in Bi-2201 to a proposed charge-stripe instability [16]. These are additional reasons to

seek still-missing direct experimental evidence for stripes in BSLCO or Bi-2201, which might correlate with our observed insulating phase.

To summarize, we measure the in-plane resistivity of BSLCO crystals down to low temperatures by suppressing superconductivity with 60-T pulsed magnetic fields. We find that metallic behavior gradually changes to insulating behavior with decreasing carrier concentration. This metal-to-insulator crossover in BSLCO takes place in the underdoped regime, at hole doping $p \sim 1/8$, in striking contrast to the behavior reported for LSCO and PCCO. Thus, the MI crossover in cuprates is not universally associated with optimum doping. On the other hand, ρ_{ab} in the insulating regime displays the clearest $\log(1/T)$ temperature dependence yet observed, suggesting a peculiar charge localization that is common in all the cuprates.

* To whom correspondence should be addressed. E-mail: ando@criepi.denken.or.jp.

† Present Address: Nichia Corporation, Kaminaka-cho, Anan-shi, Tokushima 774-8601, Japan.

- [1] P. W. Anderson, *Science* **256**, 1526 (1992).
- [2] Y. Ando *et al.*, *Phys. Rev. Lett.* **75**, 4662 (1995).
- [3] G. S. Boebinger *et al.*, *Phys. Rev. Lett.* **77**, 5417 (1996).
- [4] P. Fournier *et al.*, *Phys. Rev. Lett.* **81**, 4720 (1998).
- [5] C. Castellani, C. Di Castro, and M. Grilli, *Z. Phys. B* **103**, 137 (1997).
- [6] Y. Ando *et al.*, *J. Low Temp. Phys.* **105**, 867 (1996).
- [7] Y. Ando *et al.*, *Phys. Rev. B* **56**, R8530 (1997).
- [8] A. Maeda *et al.*, *Phys. Rev. B* **41**, 6418 (1990).
- [9] Y. Ando and T. Murayama, *Phys. Rev. B* **60**, R6991 (1999).
- [10] Y. Ando *et al.*, *Phys. Rev. Lett.* **77** 2065 (1996); **79** 2595(E) (1997).
- [11] Y. Idemoto, H. Tokunaga, and F. Fueki, *Physica C* **231**, 37 (1994), and references therein.
- [12] T. Kimura, Ph.D. Thesis, University of Tokyo (1995). Similar data can be found in H. Hwang *et al.*, *Phys. Rev. Lett.* **72**, 2636 (1996).
- [13] Y. Kubo and T. Manako, *Physica C* **197**, 378 (1992).
- [14] S.D. Obertelli, J.R. Cooper, and J.L. Tallon, *Phys. Rev. B* **46**, 14928 (1992).
- [15] One might speculate that disorder is distorting the BSCLO phase diagram, by preferentially suppressing superconductivity in the underdoped regime due to increased disorder there. If so, in cleaner samples, the maximum T_c might occur at $p \simeq 0.12$ and the MI crossover and “optimal doping” could coincide. On the other hand, we note that our interpretation, based upon our BSLCO Hall data, supports one of the most striking commonalities of the hole-doped cuprates: that optimal doping occurs at $p \simeq 0.15$.
- [16] G. Baskaran, preprint (cond-mat/9910161).
- [17] K. Yamada *et al.*, *Phys. Rev. B* **57**, 6165 (1998).